SUPPORTING INFORMATION FOR

Dysprosium-directed Metallosupramolecular Network on Graphene/Ir(111)

*Daniel Moreno,[a] Borja Cirera,[a] Sofia O. Parreiras,[a] José I. Urgel,[a] N. Giménez-Agulló,[b] Koen Lauwaet,[a] José M. Gallego,[a] J.R. Galán-Mascarós,[b,d] José I. Martínez,[*c] Pablo Ballester[*b,d], Rodolfo Miranda,[a,e] and David Écija[*a]*

[a]IMDEA Nanoscience, C/ Faraday 9, Campus de Cantoblanco, 28049 Madrid, Spain

[b]Institute of Chemical Research of Catalonia (ICIQ), The Barcelona Institute of Science and Technology, 43007, Tarragona, Spain

[c]Instituto de Ciencia de Materiales de Madrid (ICMM-CSIC), 28049 Madrid, Spain

[d]Catalan Institution for Research and Advanced Studies (ICREA), Passeia Lluis Companys 23, Barcelona 08010, Spain

[e]Departamento de Física de la Materia Condensada. Facultad de Ciencias, Universidad Autónoma de Madrid, 28049 Madrid, Spain

1. Experimental methods

The experiments were performed at IMDEA Nanoscience in a customized ultra-high vacuum chamber with a base pressure below 1 x 10^{-10} mbar. Scanning tunneling microscopy (STM) measurements have been done using a low-temperature Omicron STM operated at cryogenic temperature (4.3 K). All images have been taken in constant current mode with the V_{bias} applied to the sample, using electrochemically etched tungsten tips. Low Energy Electron Diffraction (LEED) measurements where performed with a SPECS ErLEED 150. The Au(111) sample was prepared by repeated cycles of standard Ar^+ sputtering (1.5 kV) and subsequent annealing to 723 K during 10 minutes. To prepare the graphene/Ir(111) sample, the Ir(111) was prepared by cycles of Ar^+ sputtering (1.5 kV) and flash annealing to close to 1600 K, as monitored by a pyrometer Optris, model CTlaser 3M. Graphene is obtained by chemical vapor deposition (CVD) by exposing the Ir(111) held at 1440 K to an ethene atmosphere (P_{ethene} = 3 x 10^{-7} mbar) during 6 minutes.

In order to grow the samples we tested different growth conditions and the reported results are the best networks we could design according to the protocol described in the following.

The preparation of the supramolecular architectures based on Dy-ligand coordination on metal (graphene) is achieved by a two (three) steps process:

(1) BCNB molecular ligands were deposited by organic molecular beam epitaxy from a quartz crucible held at 513 K (Kentax TCE-BSC) onto the substrate held at room temperature (300 K).
(2) For the Dy lattices: Dy atoms were evaporated employing a commercial evaporator Focus EFM3Ts using a degassed Dy rod. During deposition, the substrate was held at 340 K to favour the diffusion of both the molecules and the Dy atoms. Additionally, the substrate is post annealed at the same temperature during 3 minutes in order to grow the system in thermodynamic equilibrium conditions.[1]
(3) In the case of graphene/Ir(111), the deposition was followed by an additional annealing up to 470 K during 10 minutes to allow the formation of the Dy network.

Atomistic models showed in this work have been obtained by optimizing the BCNB molecular structure in gas phase in HyperChem software package[2] (MM+ method) and imposing it on STM images calibrated with atomic resolution images of the Au(111). Thanks to this approach we have establish the nature of the coordination node, i.e. 4-fold, 5-fold or 6-fold. Projected distances have been calculated from these models, measuring the distances from the metal atom in the coordination node to the nitrogen atoms of the surrounding ligands. These distances have been measured in several nodes to have enough statistics to obtain the averaged bond length.

Due to limitations of the tip stability and to enhance the resolution, for the analysis of the data of Dy-directed metallosupramolecular networks on gr/Ir we acquired 50 nm x 50 nm images and averaged our conclusions from those images.

2. Theoretical calculations

Ab initio calculations for the determination of the Dy-BCNB on Au(111) and Dy-BCNB on graphene/Ir(111) interfacial structures have been performed by Density Functional Theory (DFT) as implemented in the plane-wave QUANTUM ESPRESSO simulation package.[3] One-electron wave-functions are expanded in a plane-waves basis with energy cutoffs of 500 and 600 eV for the kinetic energy and the electronic density, respectively. Exchange and Correlation (XC) effects have computed in the revised generalized gradient corrected approximation (GGA) PBESol.[4,5] Kresse-Joubert Projector Augmented Wave (KJPAW) pseudopotentials[6] have been adopted to model the ion–electron interaction for all involved atoms (H, C, N, Au and Dy). In order to theoretically obtain the experimentally observed five-fold Dy—BCNB coordination 20 valence electrons have been accounted for the Dy atom, which permits to include the role of the lanthanoid $4f^{10}$ electrons in the subtle interfacial chemistry. In all calculations, Brillouin zones (BZ) have been sampled using optimal Monkhorst–Pack grids.[7] A perturbative van der Waals (vdW) correction was used to check the reliability of the adsorbed molecular ad-layer configurations. For this purpose, we have used an empirical vdW R^{-6} correction to add dispersive forces to conventional density functionals (DFT+D3).[8] Spin-polarized fashion has been considered in all calculations. Atomic relaxations were carried out using a conjugate gradient minimization scheme until the maximum force on any atom was lower than 0.02 eV/Å. The Fermi level was smeared out using the Methfessel–Paxton approach[9] with a Gaussian width of 0.01 eV, and all energies were extrapolated to T=0 K. Self-consistency in the electron density was converged to a precision in the total energy better than 10^{-6} eV. First, the clean substrates under study — Au(111) and graphene (Gr) — were fully relaxed (lattice and structure simultaneously) before considering the Dy atoms and BCNB molecules deposited on them following the adlayer arrangement obtained in the experiments for their subsequent structural optimization. Gr has been accounted as an infinite pristine graphene sheet (effect of the moire induced by the Ir(111) seems not to be important in the molecular network), and the Au(111) surface has been modeled as an infinite and periodic three-Au(111)-layer slab. For both Dy-BCNB on Au(111) and Dy-BCNB on graphene/Ir(111) interfaces a minimum perpendicular-to-the-surface distance of 20 Å has been considered in order to avoid any possible interaction between perpendicular neighboring cells.

The whole version of the BCNB molecules was used to perform all the calculations. In a first step, we pre-relaxed the gas-phase structure of the molecule to, after that, locate the optimized structure as a good geometrical starting point on the surfaces on a large battery of different molecular adlayer arrangements in interaction with the pre-deposited Dy atoms on both Au(111) and Gr. At this point, we would like to remark that, closely following the available distances and angles obtained from the experimental evidence, we tested, for both mononuclear and binuclear Dy nodes, many different interfacial configurations described as follows:

i.- Four different hexagonal lattices, each with two BCNB molecules (see figure below), for both Au (with lattice parameters ranging between 25.3 and 30.3 Å, and angles ranging between 59.7º and 60.3º) and Gr surfaces (with lattice parameters ranging between 26.4 and 31.5 Å, and angles ranging between 59.4º and 60.5º), which could perfectly hold within the experimental error in the measuring of distances and angles.

ii.- Four different on-surface adsorption sites for the mononuclear and binuclear Dy cases on Au(111) ("on-top", "on-bridge", "on-fcc-hollow", "on-hcp-hollow" sites in Au), taking into account the measured experimental Dy-Dy distance of around 4.5 $\pm$ 0.5 Å in the binuclear Dy nodes.

iii.- Finally, three different on-surface adsorption sites for the mononuclear and binuclear Dy cases on Gr ("on-top", "on-bridge", "on-hollow" sites in Gr), also taking into account the measured experimental Dy-Dy distance of around 4.5 $\pm$ 0.5 Å in the binuclear Dy nodes.

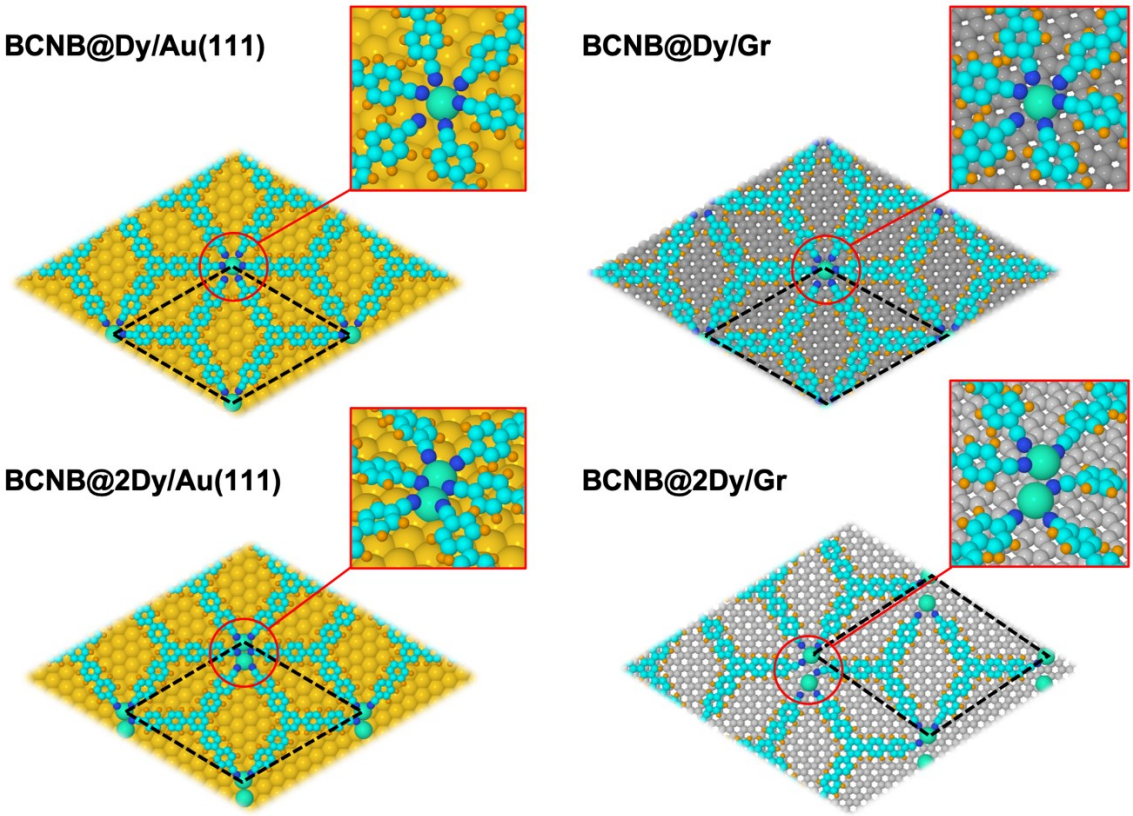

Figure S1. Pictorial views of the optimized BCNB/Dy@Au(111) and BCNB/Dy@Gr interfacial models proposed for both mono- and binuclear Dy node scenarios. Unit cell used in the calculations for each interface is indicated as a dashed-line polygon. For a better visualization zoomed insets of the Dy-node region are also shown in the figure.

Among all the lattices tested for all the mono- and binuclear Dy nodes scenarios, the energetically most stable ones, which also match with the experimentally observed 5-fold coordination in the mononuclear Dy node configuration in both Au and Gr, are those shown in the figure above, where for sake of clarity we also indicate the unit cell used in the calculations as dashed-line polygons. At this point it is important to mention that, for each lattice tested, the different calculations with different starting-points initially locating the Dy atoms on different on-surface adsorption sites always led to the same final configurations after the geometrical optimization, which are Au(111) and Gr "on-hollow" sites. Resulting candidate interfaces shown in the figure, predicted by theory also as the most stable ones, have lattice parameters of:

i.- 26.1 and 28.7 Å for mono- and binuclear nodes on Au(111), respectively, to be compared with the average value of 26.3 Å for the mononuclear Dy nodes, showing an excellent agreement with experiment.

ii.- 27.7 and 29.4 Å, for mono- and binuclear nodes on Gr, respectively, to be compared with the average experimental values of 28.3 and 28.7 Å, respectively, also with an excellent agreement.

Besides, for sake of comparison between the different configurations we have also characterized the energetics of each interfacial model analyzed. This strategy can be followed in several ways but, in our case, we have computed the average adsorption energy per molecule to the different Dy@Au and Dy@Gr systems, considered as substrates. For that purpose, we have calculated the adsorption energy per molecule as:

$$E_{ads}/molecule = \frac{\left[E_{tot}(BCNB/Dy@(Au/Gr)) - N \times E_{tot}(BCNB) - E_{tot}(Dy@(Au/Gr))\right]}{N},$$

where $E_{tot}(BCNB/Dy@(Au/Gr))$ is the total energy computed for the whole relaxed systems, *N* is the number of BCNB molecules per unit cell (in our case always is *N*=2), $E_{tot}(BCNB)$ is the total energy of a gas-phase BCNB molecule, and $E_{tot}(Dy@(Au/Gr))$ is the total energy of the substrate (with the same geometry than in the whole interfacial model). Results of the calculations reveals average adsorption energies per molecule for the most energetically stable configurations (shown in the figure above) of 3.94 and 4.72 eV (1.97 and 2.36 eV per N—Dy bond in average) for the mono- and binuclear Dy nodes configurations on Au(111), respectively, and 4.32 and 4.94 eV (2.16 and 2.47 eV per N—Dy bond in average) for the mono- and binuclear Dy nodes configurations on Gr. Notice that the effect of the vdW interaction on each substrate, by construction, is included in these energies, and can be taken as a good measure of the stability of the formed interfaces. Besides, regarding the theoretical DFT-based computation of energies, and among all the configurations tested, optimized systems with lattice parameters larger than the lowest-energy ground-state configuration will lead to a non-optimal under-connection (or under-coordination) between the molecules and the Dy atoms so decreasing the adsorption energy per molecule, and systems with lattice parameters shorter than the lowest-energy ground-state configuration will lead to a non-efficient over-connection (or over-coordination) between the molecules and the Dy atoms, as well as to fictitious induced molecular distortions, which also will lead to a decreasing the adsorption energy per molecule.

3. Comparative models of minority nodes on Dy-BCNB/Au(111).

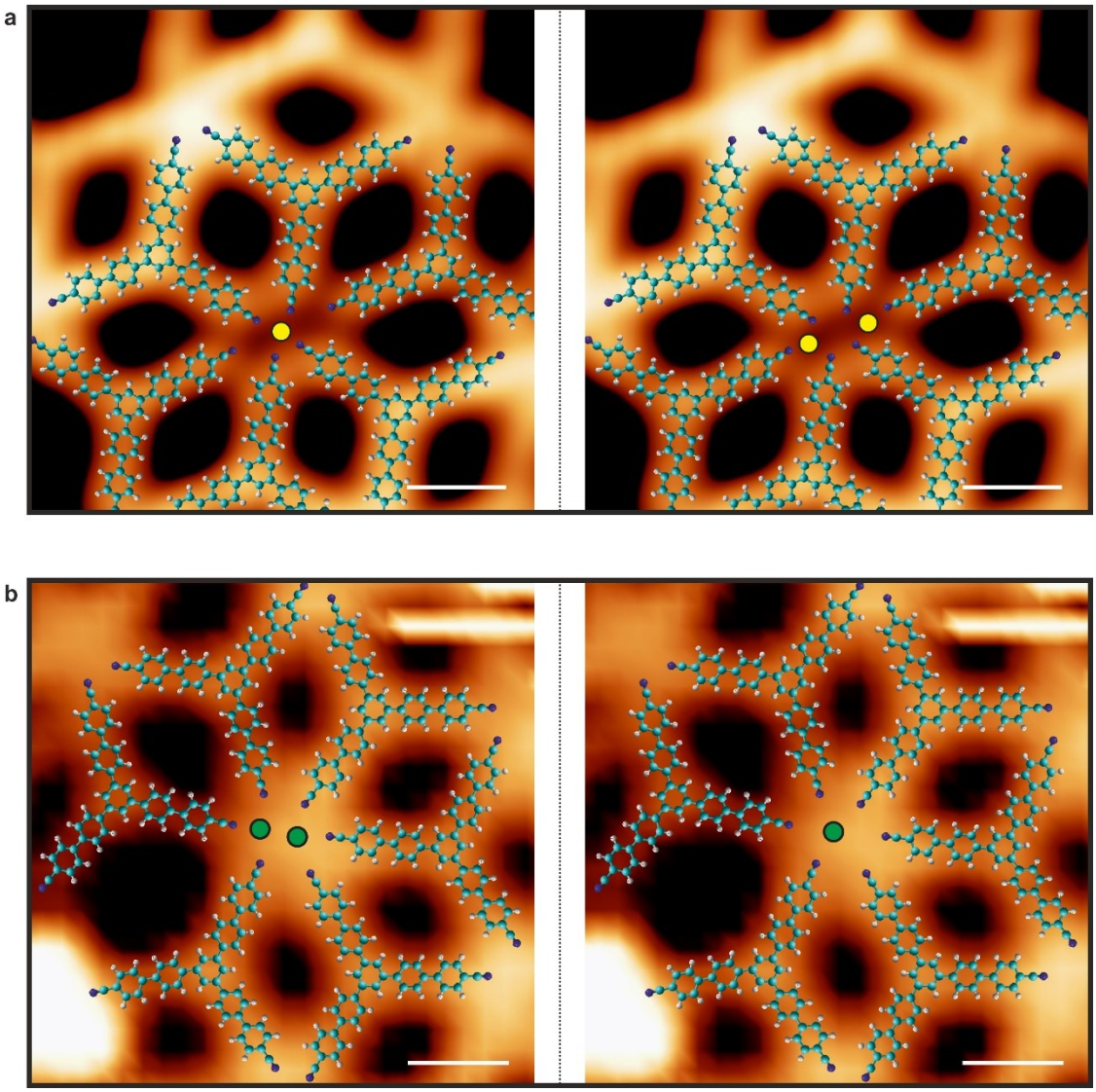

Figure S2. Modelling of minority coordination nodes of the γ phase. (a) Left: model as presented in the main manuscript. Right Alternative model for 4-fold Au node. b) Left: model as presented in the main manuscript. Right: Alternative model for binuclear 6-fold Dy node. Scanning parameters: V_b = 0.5 V, I_t = 15 pA. Scale bars: 1 nm

An exhaustive experimental modelling has been performed in order to confirm the nature of the minority coordination nodes in γ phase.

In the case of the so-called 4-fold node (Figure S2a, left panel), the STM image could suggest the feasibility of coordination with two gold adatoms (Figure S2a, right panel). Such a coordinative scheme would imply a CN···Au bond length of 1.9 ± 0.5 Å, which is in the range for that type of bonds.[10] However, in the resulting coordinative scheme some carbonitriles are now pointing away from the coordination metal centres. This would be unprecedent and, thus, very unlikely.

For the so-called Dy binuclear node (Figure S2b, left panel), an alternative configuration could be a Dy mononuclear centre (Figure S2b, right panel). However, this configuration is rapidly discarded, as for a mononuclear centre the CN···Dy bond length would be 4.5 ± 0.5 Å, which is too large when compared to reported coordination bonds.[11]

4. Randomly acquired STM images of Dy-BCNB structures on Au(111) and graphene/Ir(111)

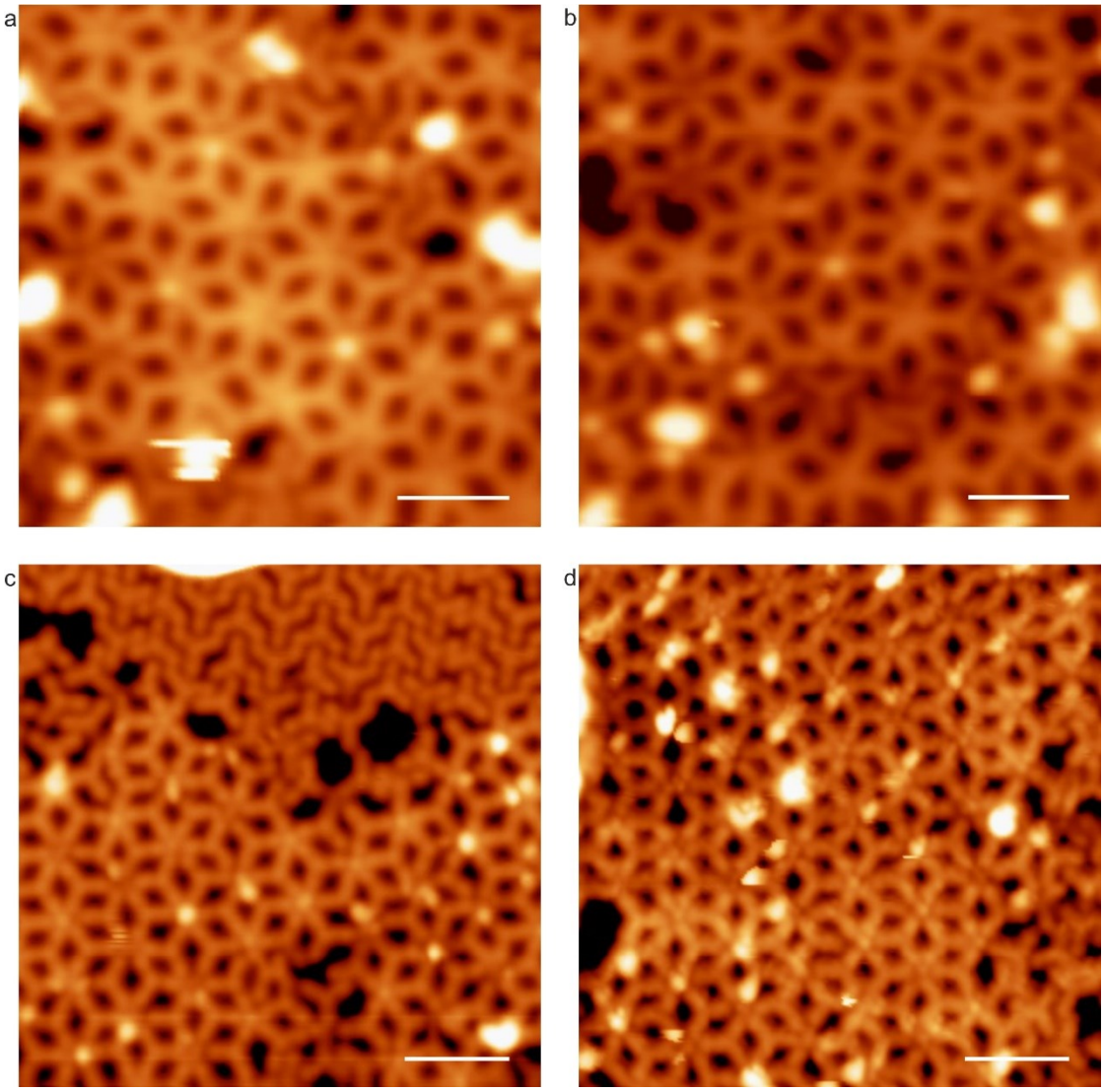

Figure S3: Dy-BCNB structures on Au(111) and Gr/Ir(111). (a) and (b) STM images of Dy-BCNB metal-organic coordination network on Au(111). Scanning parameters: (a) V_b = 1.0 V, I_t = 25 pA. Scale bar: 3 nm, (b) V_b = 1.0 V, I_t = 25 pA. Scale bar: 3 nm. (c) and (d) STM images of Dy-BCNB metal-organic coordination network on Graphene/Ir(111). Scanning parameters: (c) V_b = -1.0 V, I_t = 5 pA. Scale bar: 4 nm, (d) V_b = 0.5 V, I_t = 10 pA. Scale bar: 4 nm

5. Characterization of the graphene/Ir(111) substrate

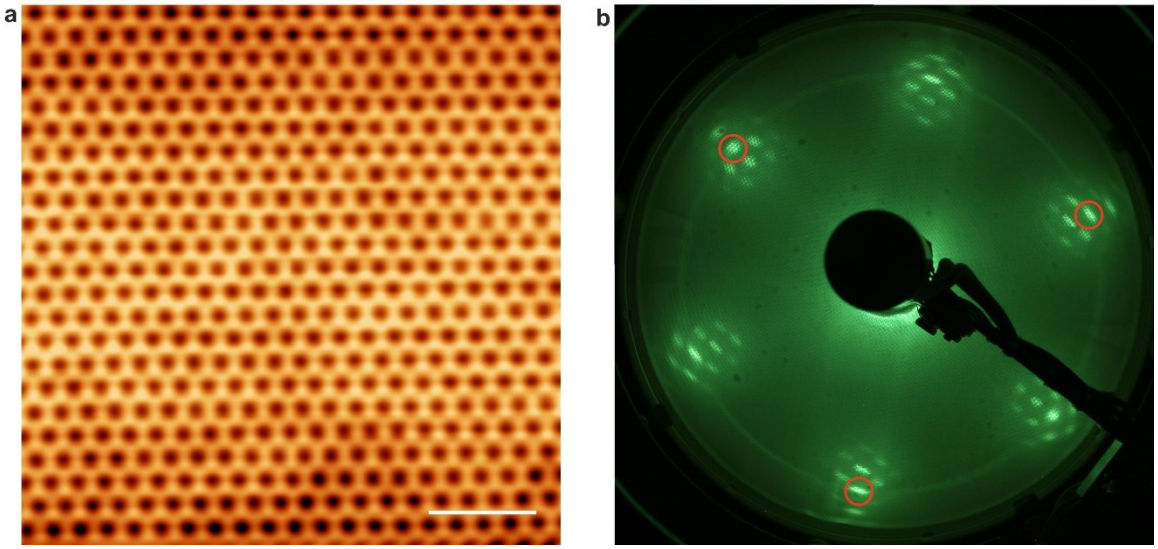

Figure S4: STM and LEED characterization of Gr/Ir(111). (a) STM image of the Moiré pattern of graphene grown on Ir(111). Scanning parameters: V_b = 5.0 V, I_t = 20 pA. Scale bar: 10 nm (b) LEED pattern of the graphene/Ir(111) substrate (at 67 eV). First order Ir(111) spots are marked with red circles.

After growing graphene on Ir(111), the crystalline quality is checked by employing both STM and LEED. In the real space the surface is fully covered by a highly perfect graphene layer, and a closer look to the substrate (Figure S3a) makes possible to appreciate the characteristic Moiré pattern produced by the lattice mismatch between graphene and the iridium crystal under it. The periodicity of this pattern is 2.49 ± 0.05 nm, in good agreement with previous experimental results[12].

Additionally, the LEED pattern (Figure S3b) shows the known Moiré pattern as clear satellite spots surrounding the first order spots associated with the Ir(111) substrate.[12,13]

6. Discussion about the intercalation of Dy on graphene/Ir (111).

Many metal atoms intercalate efficiently below graphene for distinct graphene/metal substrate combinations. Thus, it is important to verify that this is not the case for Dy deposited on the molecular network self-organized on Gr/Ir(111). In our case, the metal-organic samples on Gr/Ir(111) were grown by dosing minute amounts of Dy on the Gr/Ir(111) substrate precovered with the molecular adlayer, being held at 340 during Dy deposition, followed by annealing at 470 K for 10 minutes. The dosage of Dy was kept identical to the one used for designing coordinative networks on Au(111).

The dosage and annealing temperatures were kept well below the ones at which, recently, other rare earths, such as Eu and Hf have been shown to intercalate under Gr/Ir(111) (720 K for Eu and 670 K for Hf).[14,15]

Since Dy is directly located in the periodic table between Eu and Hf, and taking into account the minute amount of Dy deposited on Gr/Ir(111), while still giving rise to the desired metal-organic networks, we exclude the possibility of an appreciable intercalation at the annealing temperature of 470 K that could affect the substrate on which the coordinative architectures are grown.

References

1 J. V. Barth, G. Costantini and K. Kern, *Nature*, 2005, **437**, 671–679.

2 HyperChem(TM) Professional 7.51, Hypercube, Inc., 1115 NW 4th Street, Gainesville, Florida 32601, USA

3 P. Giannozzi, S. Baroni, N. Bonini, M. Calandra, R. Car, C. Cavazzoni, D. Ceresoli, G. L. Chiarotti, M. Cococcioni, I. Dabo, A. Dal Corso, S. De Gironcoli, S. Fabris, G. Fratesi, R. Gebauer, U. Gerstmann, C. Gougoussis, A. Kokalj, M. Lazzeri, L. Martin-Samos, N. Marzari, F. Mauri, R. Mazzarello, S. Paolini, A. Pasquarello, L. Paulatto, C. Sbraccia, S. Scandolo, G. Sclauzero, A. P. Seitsonen, A. Smogunov, P. Umari and R. M. Wentzcovitch, *J. Phys. Condens. Matter*, 2009, **21**, 39.

4 L. A. Constantin, J. P. Perdew and J. M. Pitarke, *Phys. Rev. B - Condens. Matter Mater. Phys.*, 2009, **79**, 1–7.

5 J. P. Perdew, A. Ruzsinszky, G. I. Csonka, O. A. Vydrov, G. E. Scuseria, L. A. Constantin, X. Zhou and K. Burke, *Phys. Rev. Lett.*, 2008, **100**, 1–4.

6 D. Joubert, *Phys. Rev. B - Condens. Matter Mater. Phys.*, 1999, **59**, 1758–1775.

7 H. J. M. James D. Pack, *J. Chem. Inf. Model.*, 1977, **16**, 1748–1749.

8 S. Grimme, J. Antony, S. Ehrlich and H. Krieg, *J. Chem. Phys.*, 2010, **132**, 154104.

9 M. Methfessel and A. T. Paxton, *Phys. Rev. B*, 1989, **40**, 3616–3621.

10 T. A. Pham, F. Song, M. N. Alberti, M. T. Nguyen, N. Trapp, C. Thilgen, F. Diederich and M. Stöhr, *Chem. Commun.*, 2015, **51**, 14473–14476.

11 J. V. Barth, *Annu. Rev. Phys. Chem.*, 2007, **58**, 375–407.

12 A. T. N'Diaye, J. Coraux, T. N. Plasa, C. Busse and T. Michely, *New J. Phys.*, 2018, **10**, 042033.

13 J. Li, L. Solianyk, N. Schmidt, B. Baker, S. Gottardi, J. C. Moreno Lopez, M. Enache, L. Monjas, R. Van Der Vlag, R. W. A. Havenith, A. K. H. Hirsch and M. Stöhr, *J. Phys. Chem. C*, 2019, **123**, 12730–12735.

14 L. Li, Y. Wang, L. Meng, R. Wu and H.-J. Gao, *App. Phys. Lett.,* 2013, **102**, 093106.

15 S. Schumacher, D. Förster, M. Rösner, T. O. Wehling and T. Michely, *Phys. Rev. Lett.,* 2013, **110**, 086111.